Journal of Colloid and Interface Science **232,** 389–399 (2000)
doi:10.1006/jcis.2000.7231, available online at http://www.idealibrary.com on IDEAL®

A Combined Pore Blockage and Cake Filtration Model for Protein Fouling during Microfiltration

Chia-Chi Ho and Andrew L. Zydney[1]

Department of Chemical Engineering, University of Delaware, Newark, Delaware 19716

Received May 25, 2000; accepted September 18, 2000

Previous studies of protein fouling during microfiltration have shown significant discrepancies between filtrate flux data and predictions of the classical pore blockage, pore constriction, and cake filtration models. A new mathematical model was developed for the filtrate flux which accounts for initial fouling due to pore blockage and subsequent fouling due to the growth of a protein cake or deposit over these initially blocked regions. The model explicitly accounts for the inhomogeneity in the cake layer thickness over different regions of the membrane arising from the time-dependent blockage of the pore surface. The model was shown to be in excellent agreement with experimental data obtained during the stirred cell filtration of bovine serum albumin solutions through polycarbonate track-etched microfiltration membranes over the entire course of the filtration. The model provides a smooth transition from the pore blockage to cake filtration regimes, eliminating the need to use different mathematical formulations to describe these two phenomena. In addition, the model provides the first quantitative explanation for some of the unusual observations reported previously in investigations of protein microfiltration. The results provide important insights into the underlying mechanisms of protein fouling during microfiltration.

Key Words: **microfiltration; protein fouling; filtration; fouling.**

INTRODUCTION

Membrane microfiltration is currently used for clarification and sterile filtration of many pharmaceutical and biotechnology products. One of the critical factors governing the overall performance of these processes is the irreversible alteration in the membrane caused by protein fouling. Previous studies of protein fouling have generally employed one of the classical fouling models: pore blockage, pore constriction, or cake filtration. A number of different functional forms have appeared in the literature for these fouling models. However, the governing equations can all be conveniently written in a common mathematical form as (1, 2)

$$\frac{d^2t}{dV^2} = k\left(\frac{dt}{dV}\right)^n \qquad [1]$$

or

$$\frac{dJ}{dt} = -kJ(JA_0)^{2-n}, \qquad [2]$$

where t is the filtration time, V is the total filtered volume, and $J = \frac{1}{A_0}\frac{dV}{dt}$ is the filtrate flux. The exponent n characterizes the filtration model, with $n = 0$ for cake filtration, $n = 1$ for intermediate blocking, $n = 3/2$ for pore constriction (also called standard blocking), and $n = 2$ for complete pore blocking.

Experimental data for the flux decline during protein filtration have often been analyzed using these simple fouling models, although there is still considerable controversy regarding the most appropriate fouling mechanism. For example, Bowen and Gan (3) analyzed their data for fouling of capillary pore aluminum oxide membranes by bovine serum albumin (BSA) solutions using a pore constriction model. Hlavacek and Bouchet (4) found good agreement between the intermediate blocking model and their data for the pressure rise during a constant flux filtration experiment. Kelly and Zydney (5) used a modified form of the pore blockage model to describe BSA fouling over a wide range of pressures and bulk protein concentrations.

More extensive studies of protein fouling have often reported a transition in fouling mechanism during the course of the filtration. For example, Tracey and Davis (6) examined the flux decline behavior during BSA microfiltration by evaluating the total resistance to filtrate flow,

$$R_{\text{total}} = \frac{\Delta P}{\mu J}, \qquad [3]$$

where μ is the solution viscosity and ΔP is the transmembrane pressure. Tracey and Davis showed that a plot of R_{total} as a function of time is concave up when $n > 1$ and is concave down when $n \leq 1$. The flux decline data for BSA were found to be consistent with either a pore constriction or a pore blockage mechanism at short times ($n > 1$), while the behavior at long times was governed by a cake filtration mechanism with $n \approx 0$. Bowen *et al.* (7) obtained similar results using an analysis based directly on Eq. [1]. In this case, the filtrate flux data at early times yielded an exponent of $n \approx 2$ on a plot of $\frac{d^2t}{dV^2}$ versus $\frac{dt}{dV}$, consistent with a pore blockage mechanism. The data at longer

[1] To whom correspondence should be addressed. Fax: 302-831-1048. E-mail: zydney@che.udel.edu.

0021-9797/00 $35.00

times suggested a cake filtration model, with n approaching zero and in some cases attaining a negative value.

Although these experimental studies provide evidence for a transition in fouling mechanism from pore blockage to cake formation, there is currently no theoretical model capable of quantitatively describing this transition using a single mathematical expression. The objective of this study was to develop a new fouling model capable of explaining filtrate flux data over the entire filtration process, accounting for both pore blockage and cake filtration. This model was verified using experimental data obtained during the constant pressure filtration of bovine serum albumin through track-etch polycarbonate membranes over a range of bulk protein concentrations and transmembrane pressures.

MODEL DEVELOPMENT

Several studies have demonstrated that protein fouling during microfiltration occurs primarily by the deposition of large protein aggregates on the membrane surface (8). Kelly and Zydney (9) showed that BSA aggregates were formed by intermolecular disulfide bonds between albumin molecules. These disulfide linkages have been identified in the aggregation of a wide range of proteins (10). Initially, these aggregates will deposit on the bare membrane, reducing the area available for unhindered filtration. This initial deposit is assumed to be at least partially permeable to fluid flow, i.e., there is some small finite flow through even the "blocked" pores. As the membrane surface becomes more heavily fouled, the protein aggregates will also begin to deposit directly on the fouling layer, causing an increase in the hydraulic resistance to flow associated with the protein deposit. This is exactly what occurs in the classical cake filtration model, although this "cake growth" is now assumed to occur simultaneously with the coverage (or blockage) of the remaining open area of the membrane.

The volumetric filtrate flow rate through the fouled membrane can thus be expressed as the sum of the flow rates through the open and blocked pores:

$$Q = Q_{\text{open}} + Q_{\text{blocked}}. \qquad [4]$$

Q_{open} is easily evaluated in terms of the clean membrane resistance (R_{m}) as

$$Q_{\text{open}} = \frac{\Delta P}{\mu R_{\text{m}}} A_{\text{open}}, \qquad [5]$$

where A_{open} is the area of the membrane which remains uncovered at any given time. The volumetric flow rate through the blocked pores is written as

$$Q_{\text{blocked}} = \int_{A_{\text{blocked}}} \frac{\Delta P}{\mu(R_{\text{m}} + R_{\text{p}})} dA, \qquad [6]$$

where R_{p} is the resistance of the protein deposit over a particular region of the membrane. Equation [6] is expressed as an integral over the blocked area to account for the spatial inhomogeneity in the resistance of the protein deposit arising from the time-dependent blockage of the membrane surface. Thus, the protein deposit on a given region of the membrane only grows over the time interval $t - t_{\text{p}}$ where t_{p} is the time at which that particular region was first covered or blocked by a protein aggregate. Those regions that have been blocked more recently will have a smaller value of R_{p} and thus a greater local filtrate flux. This is discussed in more detail subsequently.

The rate of pore coverage or blockage is assumed to be proportional to the convective flow rate of protein aggregates to the membrane surface,

$$\frac{dA_{\text{open}}}{dt} = -\alpha Q_{\text{open}} C_{\text{b}}, \qquad [7]$$

where Q_{open} is the volumetric flow rate through the open pores, C_{b} is the bulk protein concentration, and α is a pore blockage parameter which is equal to the membrane area blocked per unit mass of protein convected to the membrane surface. Each aggregate is assumed to block a given area of membrane (A_{agg}), in which case the parameter α can be expressed as

$$\alpha = \frac{f A_{\text{agg}}}{M_{\text{agg}}}, \qquad [8]$$

where f is the fractional amount of total protein present as aggregates and M_{agg} is the mass of a single aggregate. The product $f \cdot C_{\text{b}}$ is equal to the concentration (mass/volume) of protein aggregates present in the solution that are too large to pass through the membrane pores. Substitution of Eq. [5] into Eq. [7] gives a first-order ordinary differential equation for A_{open} with solution

$$A_{\text{open}} = A_0 \exp\left(-\frac{\alpha \Delta P C_{\text{b}}}{\mu R_{\text{m}}} t\right). \qquad [9]$$

The volumetric flow rate through the open pores is given directly by Eq. [5] with A_{open} evaluated from Eq. [9]. Q_{open} decreases exponentially with time at a rate which is proportional to the bulk protein concentration.

The growth of the protein deposit over each blocked region of the membrane is assumed to be proportional to the convective transport of protein through that particular region,

$$\frac{dm_{\text{p}}}{dt} = f' J_{\text{blocked}} C_{\text{b}}, \qquad [10]$$

where m_{p} is the mass of the protein deposit per unit area, and f' is the fraction of the proteins that contribute to the growth of the deposit. J_{blocked} is the filtrate flux through each region of the membrane:

$$J_{\text{blocked}} = \frac{\Delta P}{\mu(R_{\text{m}} + R_{\text{p}})}. \qquad [11]$$

The parameter f' will be equal to f under conditions where only the protein aggregates add to the deposit. f' will be greater than f if some nonaggregated protein is able to contribute to the growth of the deposit. The hydraulic resistance of the protein deposit is assumed to be directly proportional to the mass per unit area,

$$\frac{dR_p}{dt} = R'\frac{dm_p}{dt} = f'R'J_{blocked}C_b, \quad [12]$$

where the last expression is developed using Eq. [10]. R' is the specific protein layer resistance, which is assumed to be constant during a constant pressure filtration. R' will typically be a strong function of solution pH and ionic strength due to changes in the intermolecular interactions between proteins within the deposit (11). The resistance provided by the protein deposit over a given region of the membrane can be evaluated by integrating Eq. [12] using Eq. [11] to evaluate $J_{blocked}$ to give

$$R_p = (R_m + R_{p0})\sqrt{1 + \frac{2f'R'\Delta PC_b}{\mu(R_m + R_{p0})^2}(t - t_p)} - R_m, \quad [13]$$

where R_{p0} is the initial resistance of the deposit, i.e., the resistance associated with a single protein aggregate.

The total area of the membrane surface that is blocked by the protein aggregates ($A_{blocked}$) increases with time as the aggregates continue to deposit on the membrane surface,

$$dA_{blocked} = -dA_{open} = \frac{\alpha\Delta PC_b}{\mu R_m}A_0 \exp\left(\frac{-\alpha\Delta PC_b}{\mu R_m}t_p\right)dt_p, \quad [14]$$

where the last expression in Eq. [14] was obtained using Eqs. [5], [7], and [9]. Substitution of Eq. [14] into Eq. [6] yields the total volumetric flow rate through all of the blocked pores as a convolution integral over the time at which each region of the membrane was first blocked by an aggregate,

$$Q_{blocked} = Q_0\int_0^t \frac{\alpha\Delta PC_b}{\mu(R_m + R_p)}\exp\left(\frac{-\alpha\Delta PC_b}{\mu R_m}t_p\right)dt_p, \quad [15]$$

where Q_0 is the initial volumetric flow rate through the clean membrane.

Equations [4], [5], [9], and [15] can be combined to yield an expression for the filtrate flow rate through the fouled membrane at any given filtration time,

$$Q = Q_0\left[\exp\left(-\frac{\alpha\Delta PC_b}{\mu R_m}t\right) + \int_0^t \frac{\alpha\Delta PC_b}{\mu(R_m + R_p)} \times \exp\left(\frac{-\alpha\Delta PC_b}{\mu R_m}t_p\right)dt_p\right], \quad [16]$$

with R_p given as a function of t and t_p by Eq. [13]. Equation [16] thus explicitly accounts for the variation in the protein layer resistance over the surface of the membrane associated with the different time at which each region of the membrane is first blocked or covered by the protein deposit. The convolution integral in Eq. [16] can be evaluated numerically using a simple Euler integration or it can be evaluated analytically in terms of the imaginary error function. The filtrate flow rate is thus determined by the rate of pore blockage (described by the parameter α), the initial resistance of the protein deposit (R_{p0}), and the rate of increase of the protein layer resistance with time (given by the group $f'R'$).

Approximate Solution

Although Eq. [16] is relatively easy to evaluate numerically, a much simpler analytical solution can be developed for the filtrate flow rate by assuming a uniform resistance of the protein layer over the fouled surface of the membrane. Under these conditions, the coefficient multiplying the exponential in the convolution integral in Eq. [16] is a constant and can be pulled outside of the integral to give

$$Q = Q_0\left[\exp\left(-\frac{\alpha\Delta PC_b}{\mu R_m}t\right) + \frac{R_m}{R_m + R_p} \times \left(1 - \exp\left(-\frac{\alpha\Delta PC_b}{\mu R_m}t\right)\right)\right]. \quad [17]$$

The first term in Eq. [17] is equivalent to the classical pore blockage model and gives a simple exponential decay in the volumetric flow rate. At long times ($t \gg \frac{\mu R_m}{\alpha\Delta PC_b}$), the volumetric flow rate is dominated by the second term and is thus proportional to the ratio of the membrane resistance to the total resistance. The maximum value of the protein layer resistance at any time t is given by Eq. [13] with $t_p = 0$, i.e., the maximum resistance occurs over the region where the deposit has continued to grow throughout the filtration:

$$R_p = (R_m + R_{p0})\sqrt{1 + \frac{2f'R'\Delta PC_b}{\mu(R_m + R_{p0})^2}t} - R_m. \quad [18]$$

Equation [18] can be used to evaluate R_p in Eq. [17], giving a simple approximate solution for the volumetric flow rate as a function of the filtration time, t. Note that the value of Q given by Eq. [17] will always be slightly less than that given by the full numerical solution since the actual resistance of the protein layer will vary from the maximum value given by Eq. [18] to a value of R_{p0} over that region of the membrane which has just been covered by an aggregate at $t_p = t$. The use of Eq. [18] to evaluate R_p means that at long times Eq. [17] reduces to the form of the classical cake filtration model.

MATERIALS AND METHODS

Phosphate-buffered saline solutions (PBS) consisting of 0.03 M KH_2PO_4, 0.03 M $Na_2HPO_4 \cdot 7H_2O$, and 0.03 M NaOH

were prepared by dissolving preweighed quantities of the appropriate salts (Sigma, St. Louis, MO) in the desired volume of deionized water obtained from a Barnstead water purification system (Barnstead/Thermodyne, Dubuque, IA) with resistivity greater than 18 MΩcm. Solution pH was measured to within 0.01 pH units using an Acument 915 pH meter (Fisher Scientific, Pittsburgh, PA) and adjusted to 7.4 by addition of NaOH as needed. All buffer solutions were prefiltered through 0.2-μm pore size Gelman Super-200 membranes (Gelman Science, Ann Arber, MI) to remove particulates prior to use.

Bovine serum albumin solutions were prepared by dissolving crystalline BSA powder (Fraction V heat shock precipitated BSA, catalog number A7906, Sigma) in PBS. All BSA solutions were freshly prepared before each experiment and used within 8 h of preparation.

Filtration Experiments

All filtration experiments were conducted using a 25-mm-diameter stirred ultrafiltration cell (Model 8010, Amicon Corp.) connected to an acrylic solution reservoir that was air pressurized at 5.5 to 55 kPa. Data were obtained using 0.2-μm polycarbonate track-etched (PCTE) membranes obtained from Osmonics (Livermore, CA). The stirred cell and solution reservoir were initially filled with PBS, with the saline flux measured until steady state was attained (usually within 30 min). The stirred cell was then quickly emptied, refilled with a BSA solution, and attached to a fresh reservoir containing additional BSA solution. The system was repressurized (within 1 min) and the filtrate flow rate was measured by timed collection using a digital balance (Sartorious Model 1580, Edgewood, NY). At the end of the filtration, the stirred cell was rinsed with PBS, and the steady state PBS flux was reevaluated. All experiments were performed at room temperature (22 $\pm$ 2°C).

The resistance of the protein deposit formed after filtration was evaluated as follows. A single membrane was used to filter a 2 g/L BSA solution for 5 h at a constant pressure of 14 kPa (2 psi). The stirred cell was emptied, the membrane was gently rinsed with saline, and the stirred cell was then filled with a fresh PBS solution that had first been prefiltered through a 100 K Biomax (Millipore, MA) membrane. The saline flow rate was measured at several pressures, with sufficient time provided for the system to attain steady state (usually within 2 h).

The amount of protein deposited on the membrane was evaluated by direct weighing. A clean (dry) membrane was initially weighed using a Sartorious balance with an accuracy of 0.1 mg. The membrane was then used to filter a preset volume of 2 g/L BSA solution at 14 kPa. The hydraulic permeability of the fouled membrane was evaluated as described above. The membrane was then air dried for 12 h and reweighed to estimate the mass of the deposited protein.

RESULTS AND ANALYSIS

Figure 1 shows typical experimental data for the filtrate flux (top) and total collected filtrate volume (bottom) as a function of time during the constant pressure, $\Delta P = 14$ kPa (2 psi), stirred cell filtration of five different BSA solutions with concentrations ranging from 0.5 to 5 g/L. The initial flux ranged from 3.2×10^{-4} to 4.0×10^{-4} m/s due to the inherent membrane to membrane variability. These values were all within 10% of the steady-state saline flux evaluated just prior to switching to the protein solution. The flux declined quite rapidly at the start of the filtration, with the rate of flux decline increasing with increasing bulk protein concentration. At long times, the flux appeared to approach a nearly constant value which was more

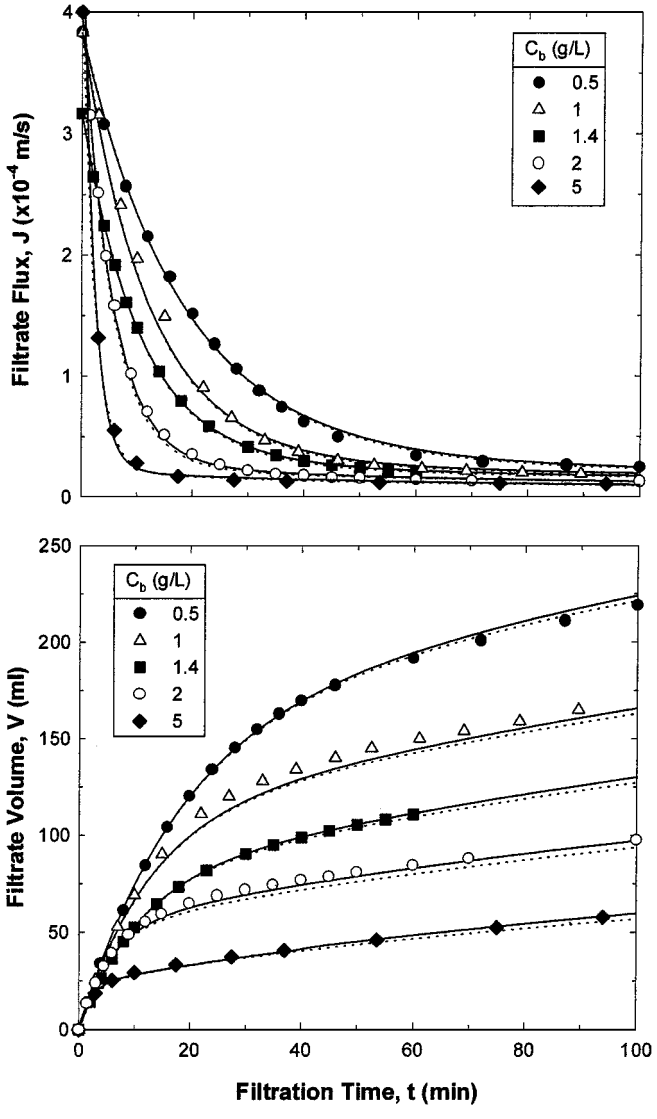

FIG. 1. Filtrate flux (top) and total filtrate volume (bottom) for BSA filtration through the PCTE membranes at 14 kPa. Solid and dotted curves are model calculations using the complete model (Eq. [16]) and the approximate analytical solution (Eq. [17]).

than an order of magnitude smaller than the initial flux. The filtrate volume is nearly independent of the bulk protein concentration at very short times where $J \approx J_0$. The curves diverge after about 5 min, with the total volume increasing with decreasing protein concentration. Although the data at long times look nearly linear on this scale, the filtrate flux continues to decline with time leading to a gradual reduction in the rate at which V increases. This is discussed in more detail subsequently. These results were highly reproducible, with the data from repeat experiments differing by less than 10%.

The solid and dotted curves in the top and bottom panels of Fig. 1 are the model calculations using Eqs. [16] and [17], respectively. The best fit values of the parameters α, R_{p0}, and $f'R'$ were determined by minimizing the sum of the squared residuals between the filtrate flux data and the calculations from the complete model (Eq. [16]) using the method of steepest descent. This yielded $\alpha = 4.1 \pm 0.2$ m^2 kg^{-1}, $R_{p0} = 4.0 \pm 0.2 \times 10^{11}$ m^{-1}, and $f'R' = 2.4 \pm 0.2 \times 10^{12}$ m kg^{-1}, with the standard deviations in the parameter values determined from the optimization routine. The model calculations are in very good agreement with the experimental data for both the filtrate flux (J) and the filtration volume (V) over the entire time interval and over the full range of bulk protein concentrations using this single set of parameters. The model accurately describes the rapid flux decline seen during the early stages of the filtration as well as the much slower rate of flux decline at long times.

Although it is not possible to quantitatively obtain independent values of these fouling parameters, we can obtain rough estimates for α and R_{p0} based on literature data for BSA. Ho and Zydney (12) estimated the fraction of protein present in these BSA solutions as aggregates as $f = 0.0003 \pm 0.0002$ using quasi-elastic light scattering. The average diameter of the protein aggregates was also determined by both light scattering and scanning electron microscopy as 0.36 ± 0.1 μm, yielding $A_{agg} = 1.1 \pm 0.6 \times 10^{-13}$ m^2 and $M_{agg} = 3.0 \pm 2.1 \times 10^{-17}$ kg using a simple hard sphere model for the aggregates. Substitution of these values into Eq. [8] gives $\alpha = 2.9 \pm 2.6$ m^2 kg^{-1}, which is in good agreement with the best fit value of $\alpha = 4.1 \pm 0.2$ m^2 kg^{-1} determined from the filtrate flux data in Fig. 1. The resistance of the initial protein deposit (R_{p0}) can be estimated from the Kozeny–Carman equation,

$$R_p = \frac{5\delta_m}{\varepsilon S^2}, \qquad [19]$$

where δ_m, ε, and S are the thickness, porosity, and specific surface area of the protein deposit. Mochizuki and Zydney (13) estimated the specific surface area of a complete BSA deposit from dextran sieving measurements as $S \approx 30$ Å. This gives $R_{p0} = 4 \times 10^{11}$m^{-1} using $\varepsilon = 0.5$ and $\delta_m = 0.36$ μm, with the latter simply equal to the size of a single aggregate. This value is nearly identical to the best fit value of R_{p0} determined previously from the filtrate flux data ($R_{p0} = 4.0 \pm 0.2 \times 10^{11}$ m^{-1}). The parameter $f'R'$ can also be estimated independently, and this will be discussed subsequently.

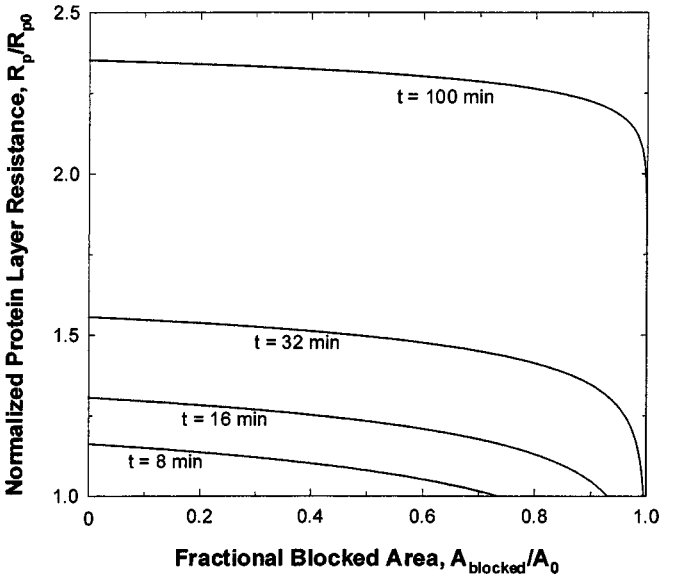

FIG. 2. Model calculations using the complete model (Eq. [16]) for the normalized protein layer resistance as a function of cumulative fractional blocked area for 2 g/L BSA filtration through the PCTE membrane at 14 kPa.

The results from the approximate analytical solution (dotted curves in Fig. 1) are only slightly below those of the full solution, even though Eq. [17] is developed by assuming a uniform (maximum) resistance of the protein deposit over the entire fouled region of the membrane. To highlight the effect of the inhomogeneity in the protein layer resistance over the membrane surface, Fig. 2 shows the calculated values of the protein layer resistance normalized by the resistance of a single aggregate (R_{p0}) as a function of the fractional blocked area at four different filtration times. The protein layer resistance at each time t was evaluated from Eq. [13] as a function of t_p, the time at which the region of the membrane surface was first covered by an aggregate. The area was then related to t_p by integration of Eq. [14] for the run with $C_b = 2$ g/L and $\Delta P = 14$ kPa. The resistance of the fouled membranes varies from the maximum value of R_p given by Eq. [18] to R_{p0} for that region of the membrane which was just covered by an aggregate at $t_p = t$. At short filtration times, a significant fraction of the membrane remains unblocked by any protein aggregates, with most of the flow going through these unblocked areas. For example, at $t = 8$ min only 6% of the total filtrate flow is through the fouled regions even though 74% of the membrane surface is covered by the protein deposit. Under these conditions, the predictions of the approximate model are nearly identical to those of the full model. The total variation in the protein layer resistance becomes more pronounced at longer filtration times, although the resistance over much of the membrane surface is fairly close to the maximum value. The reason for this is that those regions which are fouled first have the greatest resistance and thus the smallest flux, leading to the slowest rate of cake growth (Eq. [10]). The net result is that the cake growth is a self-leveling process, with those regions

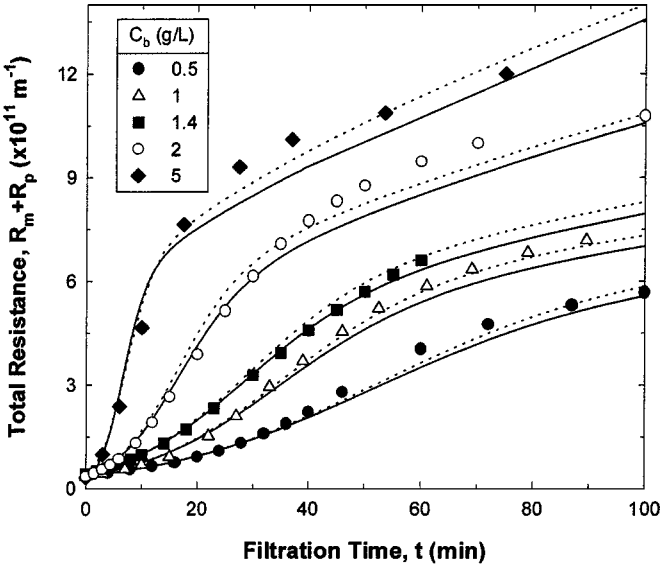

FIG. 3. Total resistance as a function of time for BSA filtration through the PCTE membranes. Solid and dotted curves are model calculations using the complete model (Eq. [16]) and the approximate analytical solution (Eq. [17]).

having greater resistance (i.e., thickness) fouling more slowly. At $t = 32$ min, the average resistance over the fouled region is only 6% smaller than the maximum resistance and this decreases to less than 3% after 100 min. This self-leveling phenomenon explains why the simple approximate solution developed with R_p equal to the maximum resistance provides such accurate predictions for the filtrate flux.

As discussed by Tracey and Davis (6), the filtrate flux data can be used to examine the underlying fouling mechanism by replotting the data in terms of the total resistance as given by Eq. [3]. The results are shown in Fig. 3, with the solid and dotted curves showing the complete model calculations and approximate solutions using the same parameter values as in Fig. 1. The total resistance data are clearly concave up during the early stage of the filtration, which is consistent with either a pore blockage or a pore constriction mechanism (6). In contrast, the data at long times are concave down, implying a cake filtration mechanism. This general behavior has been discussed previously by Tracey and Davis (6). The transition between these two phenomena, defined by the inflection point in the total resistance versus time plot, occurs at longer times for the experiments with lower bulk protein concentration. The model calculations are in good agreement with the total resistance data, although the numerical solution does tend to underestimate the resistance at long times. Better agreement at long times was attained using a slightly larger value of $f'R'$. The model accurately describes the transition in fouling mechanisms, with the initial flux decline dominated by pore blockage/coverage while the long-term fouling is due to the growth of the protein cake layer. The total resistance continues to increase even after 100 min of filtration at the highest protein concentration, indicating that the flux never attains a steady-state value under the conditions of these experiments.

An alternative approach that can be used to analyze the filtrate flux data is to replot the results as d^2t/dV^2 versus dt/dV as suggested by Eq. [1]. The required derivatives were evaluated in terms of the filtrate flux,

$$\frac{dt}{dV} = \frac{1}{JA} \qquad [20]$$

$$\frac{d^2t}{dV^2} = -\frac{1}{J^3A^2}\frac{dJ}{dt}, \qquad [21]$$

with dJ/dt evaluated numerically by differentiating the flux versus time data in Fig. 1 using IMSL routine DCSDER to take the derivative of a series of piecewise cubic polynomials that were fit to the raw data. The solid curves in Fig. 4 are the model calculations based on the approximate analytical solution (Eq. [17]) using the same parameter values as in Figs. 1 to 3. At small dt/dV, corresponding to short filtration times, the data yield a linear relationship with slope on the log–log plot equal to 2.0 $\pm$ 0.1 with a correlation coefficient of $r^2 > 0.998$. The slope $n = 2$ is exactly the behavior predicted by the classical pore blockage model. The complete model developed in this study actually predicts a slope slightly less than 2.0 due to the flow through the blocked pores. The initial slope on the log–log plot can be evaluated analytically by differentiating the logarithm of d^2t/dV^2 with respect to the logarithm of dt/dV:

$$n = \frac{d\left[\log\left(\frac{d^2t}{dV^2}\right)\right]}{d\left[\log\left(\frac{dt}{dV}\right)\right]}. \qquad [22]$$

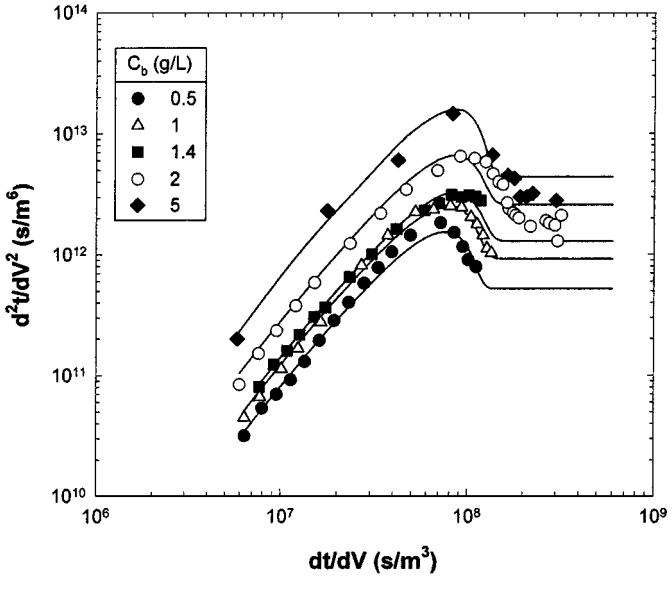

FIG. 4. Flux decline analysis for BSA filtration at different bulk protein concentrations. Experimental data are from Fig. 1. Solid curves are model calculations using Eq. [17].

The required derivatives can be evaluated using Eqs. [20] and [21] and the approximate expression for the flux (Eqs. [17] and [18]) to give the following expression for the initial slope, i.e., n evaluated at $t = 0$:

$$n = 3 - \frac{R_m + R_{p0}}{R_{p0}} + 2\frac{R_m^2}{R_{p0}^2(R_m + R_{p0})}\frac{f'R'}{\alpha}. \qquad [23]$$

Equation [23] gives $n = 1.94 \pm 0.03$ using the best fit values of the model parameters for BSA. This result is in good agreement with the experimental data. Note that Eq. [23] is strictly valid at $t = 0$, while the slope determined experimentally is actually an average value over the first few time points in the filtration.

The results in Fig. 4 display a distinct maximum in the plot of d^2t/dV^2 versus dt/dV at an intermediate filtration time at each bulk protein concentration. This type of maximum was also seen by Bowen *et al.* (7) in their study of BSA filtration through track-etched polycarbonate membranes, although they provided no quantitative explanation for this behavior. The height of the maximum increases with increasing bulk protein concentration, although the location of the maximum value for all five runs occurs at $dt/dV \approx 7.5 \times 10^7$ s/m^3, corresponding to $J/J_0 \approx 0.09$. Thus, the maximum value of d^2t/dV^2 occurs when the membrane surface is more than 90% covered by the protein aggregates. At very long times, i.e., $dt/dV > 2 \times 10^8$ s/m^3 or $J/J_0 < 0.04$, the model predicts that d^2t/dV^2 approaches a constant, i.e., the slope becomes equal to zero. This behavior corresponds to the classical cake filtration model. The asymptotic value of d^2t/dV^2 increases linearly with increasing protein concentration due to the increase in the rate of cake growth as given by Eq. [10]. The experimental data for the 5 and 2 g/L BSA solutions do show a nearly constant, or slightly decreasing, value of d^2t/dV^2 at very long times (between 1 and 10 h of filtration), although there are large uncertainties in the evaluation of the derivatives under these conditions due to the very slow rate of flux decline at long filtration times. Longer time data would be needed to see the cake filtration behavior for the runs with lower protein concentrations.

It is interesting to note that the transition between the pore blockage and cake filtration models results in a negative slope on the plot of d^2t/dV^2 versus dt/dV for the BSA filtration data. This behavior is very accurately described by our new fouling model, even though this result cannot be even qualitatively explained by any of the classical fouling models, all of which yield $n > 0$. The decrease in d^2t/dV^2 reflects the large reduction in the rate of flux decline (dJ/dt) that occurs during the transition between the pore blockage and cake filtration mechanisms, with dJ/dt decreasing much more rapidly than J during this transition period.

A more traditional approach to examine the fouling mechanism is to plot the filtrate flux data in an appropriate linearized form developed by rearranging the expressions for the classical pore blockage, pore constriction, and cake filtration models (14). Figure 5 shows the results, with the solid curves representing the

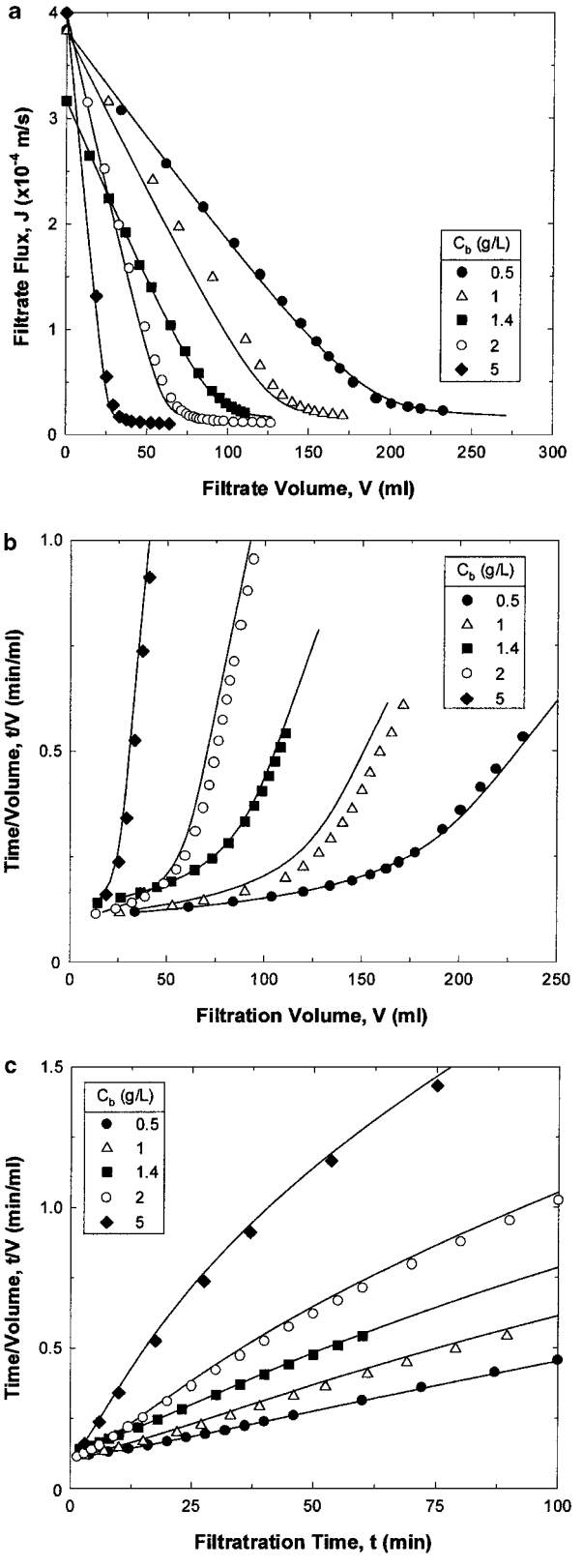

FIG. 5. Flux decline data for BSA filtration at different bulk protein concentrations plotted in accordance with (a) the pore blockage model, (b) the cake filtration model, and (c) the pore constriction model. Experimental data are from Fig. 1. Solid curves are model calculations using Eq. [17].

model calculations given by Eq. [17] using the parameter values determined previously. The classical pore blockage model (Fig. 5a) predicts that a plot of the filtrate flux (J) versus filtration volume (V) is linear, in good agreement with the data at short times where the flux is dominated by the pore blockage mechanism. However, at long times the flux data shows significant deviation from linearity due to the flux through the blocked pores. The classical cake filtration model (Fig. 5b) predicts that a plot of t/V should be linear in V, in good agreement with the data at long filtration times (large V). However, a simple linear fit to the data yields a non-zero intercept on the volume axis, which is physically unrealistic. The classical pore constriction model (Fig. 5c) predicts that t/V is linear with t, a result which is in surprisingly good agreement with the BSA data, particularly at low protein concentrations. This behavior could easily be misinterpreted as indicating that the fouling occurs by a pore constriction mechanism, even though the results from Figs. 3 and 4 clearly indicate that fouling occurs first by pore blockage and then by cake formation. Our new fouling model provides a very good description of the filtration data on all three plots, with the model calculations also appearing highly linear when plotted as t/V versus t (Fig. 5c). The linearity of the model and data using this form arises from the transition between the pure pore blockage ($n = 2$) and cake filtration ($n = 0$) mechanisms during the filtration experiment.

Figure 6 shows the effect of the transmembrane pressure drop on the filtrate flux and filtrate volume during the stirred cell filtration of 2 g/L BSA solutions. The initial flux increased approximately linearly with increasing transmembrane pressure (ΔP) since these membranes were incompressible at the low pressures (<55 kPa or 8 psi) used in these experiments. The initial rate of flux decline was quite rapid, particularly at the higher transmembrane pressure drops. The flux decreased to less than 10% of its initial value within 5 min of filtration at 8 psi compared to more than 40 min of filtration at 0.8 psi. This caused the flux at $\Delta P = 0.8$ psi to become larger than that at any of the other pressures for t between 15 and 30 min. At long filtration times, the filtrate flux differed by less than 40% over the 10-fold range of transmembrane pressure drops. The total filtrate volume was greatest for the run at the highest transmembrane pressure, although the dependence of V on ΔP was very nonlinear. Thus, at the end of the 100 min filtration, the filtrate volume for the run with $\Delta P = 2$ psi was only 27% greater than that for the run at $\Delta P = 0.8$ psi.

The solid curves in the top and bottom panels of Fig. 6 represent the model calculations from the approximate solution using the value of α determined from the data in Fig. 1 ($\alpha = 4.1 \pm 0.2$ m^2 kg^{-1}). The best fit values of the parameters R_{p0} and $f'R'$ were determined at each ΔP by minimizing the sum of the squared residuals between the experimental data in Fig. 6 and the model calculations. The corresponding calculations using the complete model (Eq. [16]) were nearly indistinguishable from the results for the approximate analytical solution (Eq. [17]) and were thus left off the graph. The best fit values

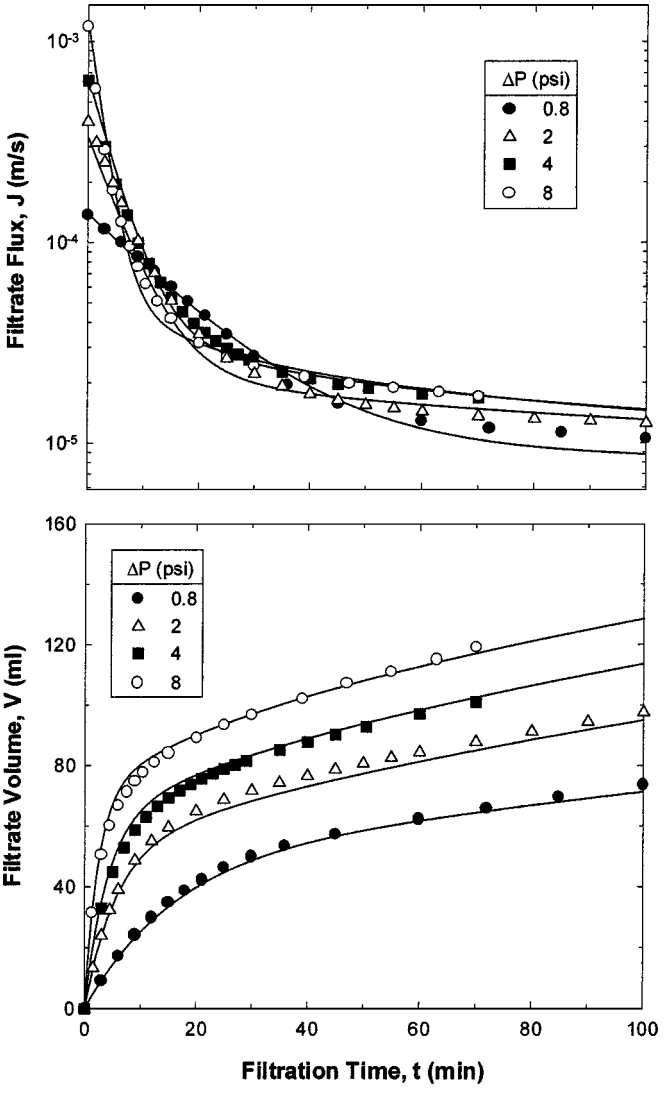

FIG. 6. Effect of transmembrane pressure on the filtrate flux (top) and filtrate volume (bottom) during filtration of 2 g/L BSA solutions. Solid curves are model calculations using Eq. [17].

for R_{p0} and R' are shown in Fig. 7 as a function of the transmembrane pressure. The initial resistance of the protein deposit ranged from 3.3×10^{11} to 4.0×10^{11} m^{-1} with no significant dependence on the transmembrane pressure. In contrast, the specific resistance of the protein layer R', evaluated from the best fit values of $f'R'$ assuming that $f' = 0.0003$ (solid circles), increases with increasing transmembrane pressure. This increase in R' is likely due to the compressibility of the BSA deposit, with the packing density of the BSA increasing with increasing pressure.

The compressibility of the protein deposit was evaluated independently by measuring the steady-state saline flux through a heavily fouled membrane as a function of the transmembrane pressure. The total resistance ($R_m + R_p$) was calculated using Eq. [3]. The protein layer resistance was obtained by simply

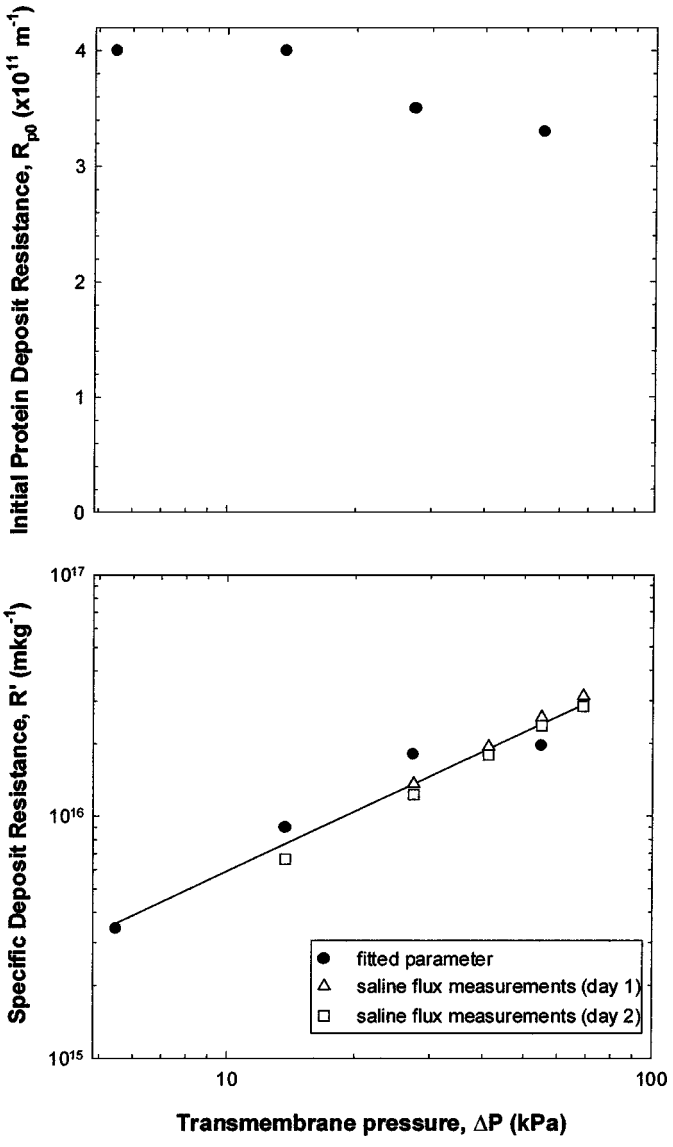

FIG. 7. Initial protein layer resistance (top) and specific protein layer resistance (bottom) as a function of transmembrane pressure. Filled circles represent the values obtained by fitting the flux data in Fig. 6. Triangles and squares are data from steady-state saline flux through a fouled membrane at different pressures. The solid line is linear regression based on Eq. [24].

subtracting off the membrane resistance (R_m), which was assumed to be unaffected by the filtration. Results are shown as the open symbols in the bottom panel of Fig. 7. The specific resistance was evaluated using Eq. [12] with the mass of the protein deposit equal to 0.15 mg as determined by direct weighing of the clean and fouled membrane. The resistance evaluated from the saline flux measurements was in very good agreement with the best fit value determined directly from the filtrate flux data. This good agreement using $f' = f = 0.0003$ indicates that the growth of the protein deposit in these experiments was due almost entirely to the deposition of the large BSA aggregates. If the monomeric BSA were able to add significantly to the protein deposit then f' would be greater than f, causing the resistance determined from the filtrate flux data using $f' = f$ to be much greater than that evaluated from the saline flux measurements. The increase in the specific resistance with increasing transmembrane pressure was completely reversible. Data obtained after soaking the membrane overnight (squares) showed nearly identical values of the steady-state saline flux over the entire pressure range.

The specific resistance data for the BSA deposit are highly linear when plotted on a log–log graph. This is consistent with the power law relationship used previously by Porter (15) and Belter *et al.* (16) to describe the compressibility of different filter cakes:

$$R' = k(\Delta P)^s, \qquad [24]$$

where k is a constant related to the size and shape of the particles within the deposit. The cake compressibility, s, varies between zero for an incompressible layer to a value of 1 for a very highly compressible layer. The best fit values of k and s were determined by simple linear regression of the data in the bottom panel of Fig. 7 yielding $s = 0.82$ and $k = 3.0 \times 10^{12}$ m kg^{-1}(m^2 N^{-1})$^{0.82}$ with $r^2 = 0.96$. The compressibility coefficient for the BSA deposit is quite high. For example, Opong and Zydney reported a value of 0.43 (17). These discrepancies could reflect differences in the BSA preparations used in these experiments, or they could be due to differences in the experimental procedures used to evaluate the specific protein layer resistance.

The filtrate flux data at the different applied pressures have been replotted in Fig. 8 as d^2t/dV^2 versus dt/dV. The solid

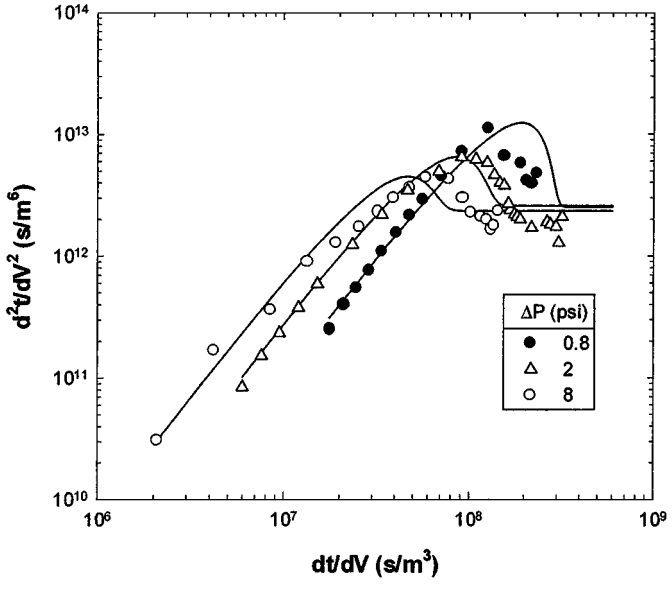

FIG. 8. Flux decline analysis for BSA filtration at different transmembrane pressures. Experimental data are from Fig. 6. Solid curves are model calculations using Eq. [17].

curves are the model calculations using Eq. [17] with the specific resistance of the protein layer evaluated from Eq. [24] using the best fit values of k and s. The data at short times (i.e., small dt/dV) are again highly linear with a slope equal to 2, consistent with the pore blockage model. Note that the data obtained at the higher transmembrane pressures start at lower values of dt/dV due to the higher initial flux. The data and model again show a distinct maximum in d^2t/dV^2 due to the transition between the pore blockage and cake filtration fouling mechanisms. In contrast to the data in Fig. 4, the location of the maximum shifts to a higher dt/dV (lower J) with decreasing pressure, although the maximum value of d^2t/dV^2 again occurs between $J/J_0 = 0.05$ and 0.1. The shift in the location of the maximum causes the curves for d^2t/dV^2 to cross at an intermediate time, before decaying to a constant value of d^2t/dV^2 at very long times where the fouling is dominated by the growth of the protein cake layer. The weak dependence of the asymptotic value of d^2t/dV^2 on the applied pressure is a direct result of the high degree of compressibility of the protein deposit.

The effects of the specific protein layer resistance on the flux decline behavior are examined in more detail in Fig. 9. Calculations are shown for the complete model (Eq. [16]—solid curves) and the approximate solution (Eq. [17]—dotted curves) for several values of R' with $\alpha = 4.1 \pm 0.2$ m^2 kg^{-1}, $R_{p0} = 4.0 \pm 0.2 \times 10^{11}$ m^{-1}, and $f' = 0.0003$ as determined previously. The results for the complete and approximate solutions are identical at very short times and for small R' since the flux is dominated by pore blockage and the initial resistance of the protein deposit under these conditions. Some discrepancies are seen at large R', with the approximate solution overpredicting d^2t/dV^2 since it underestimates the flux at any time t. The simulations with $R' \neq 0$ are similar to those seen previously in Figs. 4 and 8. The maximum value of d^2t/dV^2 increases with increasing R', and the location of the maximum is shifted to a higher value of dt/dV. Thus, as the specific resistance of the cake layer increases, the onset of the cake filtration mechanism occurs at a lower flux (i.e., at a higher dt/dV). This seemingly counterintuitive behavior arises because the flux through the blocked pores decreases rapidly when the specific cake resistance is large. The net result is that more of the flow occurs through the open pores, with the rate of flux decline determined by the rate of pore blockage out to a larger value of dt/dV corresponding to a smaller filtrate flux. The asymptotic value of d^2t/dV^2 obtained at very long times is directly proportional to R' since the flux in this region is determined entirely by the cake filtration mechanism. The behavior when the specific cake resistance is zero is somewhat different. The values of d^2t/dV^2 still show a maximum, but there is no longer any asymptotic cake filtration behavior at very long times. Instead, the filtrate flux approaches a true steady-state value given by Eq. [6] but with $R_p = R_{p0}$ over the entire membrane. The presence of a steady-state flux causes d^2t/dV^2 to approach zero at a finite value of dt/dV. This behavior will occur whenever the flux attains a steady-state value irrespective of the underlying mechanism and thus provides a very convenient graphical approach for determining the existence of a steady-state flux in any membrane process.

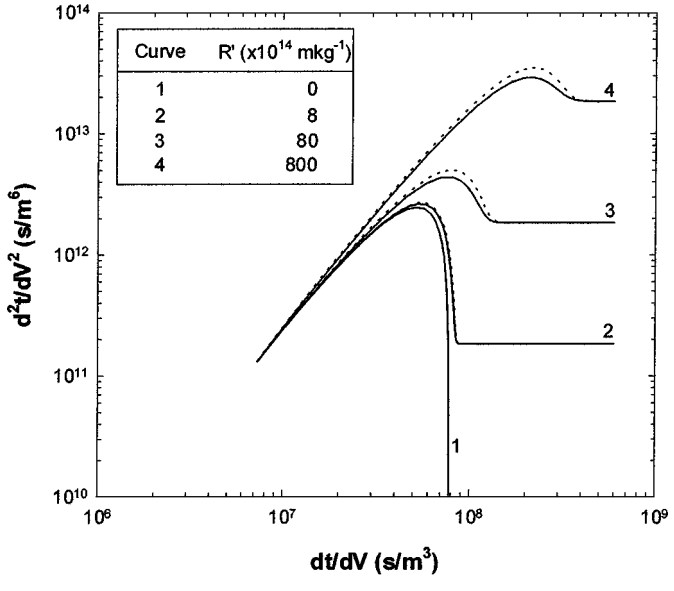

FIG. 9. Effect of specific cake resistance (R') on the flux decline. The solid and dotted curves are model calculations using the complete model (Eq. [16]) and the approximate solution (Eq. [17]) for different R'.

CONCLUSION

Although protein fouling during microfiltration has been studied quite extensively over the past 20 years, none of the existing models has been able to explain the complex range of phenomena observed experimentally. The theoretical model developed in this study provides a much more complete and rigorous description of the fouling behavior. The initial flux decline arises from pore blockage by the physical deposition of large protein aggregates on the membrane surface. Unlike most prior pore blockage models, these aggregates are assumed to allow some fluid flow through the blocked pores, with the resistance to flow over each blocked region increasing with time as additional protein is convected to the membrane surface. The model thus explicitly accounts for the spatial variation in the protein layer resistance over the membrane surface, with those regions that were fouled first having the greatest total hydraulic resistance to filtration. The model thus provides a smooth transition from the pore blockage to cake filtration behavior during the course of the filtration, eliminating the need to use completely separate mathematical descriptions in these fouling regimes. A simple approximate solution which ignores this spatial variation in the protein layer resistance was also developed and shown to be in very good overall agreement with predictions of the more complete solution due to the self-leveling behavior inherent in the cake growth process.

The model calculations were shown to be in excellent agreement with experimental data for the constant pressure filtration

of bovine serum albumin solutions over a range of bulk protein concentrations and transmembrane pressures. The specific resistance of the protein deposit (R') was a strong function of the transmembrane pressure due to the highly compressible nature of the protein deposit. Previous studies have demonstrated that the specific resistance (11) and degree of protein aggregation (9) are also functions of the solution conditions, e.g., pH and ionic strength, due to intermolecular electrostatic interactions.

The model was also able to explain the observed maximum in a plot of d^2t/dV^2 versus dt/dV, a phenomenon which has been observed previously but which has never been explained mechanistically. Although the three model parameters were evaluated from the flux decline data, they each have a clear physical meaning. Thus, in principle these parameters could all be evaluated from independent measurements of the physical characteristics of the protein aggregates and the resulting protein deposit. Experimental results for the BSA system yielded parameter values which were in very good agreement with the model fits, demonstrating the validity of this approach to describing the flux decline during protein microfiltration through membranes with noninterconnected pore structures.

APPENDIX: NOMENCLATURE

A_{agg}	Membrane area blocked by a single aggregate, m^2
$A_{blocked}$	Area of membrane blocked by protein deposit, m^2
A_{open}	Area of unblocked (clean) membrane, m^2
A_0	Total area of the membrane, m^2
C_b	Bulk protein concentration, g/L
f	Fractional amount of total protein present as aggregates
f'	Fractional amount of total protein that contributes to deposit growth
J	Filtrate flux, m/s
k	Proportionality coefficient for specific protein layer resistance, m kg^{-1} $(m^2\ N^{-1})^{0.82}$
M_{agg}	Mass of a single aggregate, kg
ΔP	Transmembrane pressure, N/m^2
Q	Volumetric flow rate, m^3/s
R_m	Resistance of the clean membrane, m^{-1}
R_p	Resistance of the protein deposit, m^{-1}
R_{p0}	Resistance of a single protein aggregate, m^{-1}
R'	Specific protein layer resistance, m/kg
s	Compressibility coefficient for protein layer
S	Specific surface area of the protein, m
t	Filtration time, s
V	Total collected filtrate volume, m^3
α	Pore blockage parameter, m^2/kg
ε	Membrane porosity
δ_m	Membrane thickness, m

ACKNOWLEDGMENTS

This work was supported in part by a grant from the National Science Foundation.

REFERENCES

1. Hermans, P. H., and Bredée, H. L. *J. Soc. Chem. Ind.* **55T,** 1 (1936).
2. Gonsalves, V. E., *Rec. Trav. Chim. des Pays-Bas* **69,** 873 (1950).
3. Bowen, W. R., and Gan, Q., *Biotech. Bioeng.* **38,** 688 (1991).
4. Hlavacek, M., and Bouchet, F., *J. Membrane Sci.* **82,** 285 (1993).
5. Kelly, S. T., and Zydney, A. L., *J. Membrane Sci.*, **107,** 115 (1995).
6. Tracey, E. M., and Davis, R. H., *J. Colloid Interface Sci.* **167,** 104 (1994).
7. Bowen, W. R., Calvo, J. I., and Hernández, A., *J. Membrane Sci.* **101,** 153 (1995).
8. Kelly, S. T., Opong, W. S., and Zydney, A. L., *J. Membrane Sci.* **80,** 175 (1993).
9. Kelly, S. T., and Zydney, A. L., *Biotech. Bioeng.* **44,** 972 (1994).
10. Liu, W. R., Langer, R., and Klibanov, A. M., *Biotech. Bioeng.* **37,** 177 (1991).
11. Palecek, S. P., and Zydney, A. L., *J. Membrane Sci.* **95,** 71 (1994).
12. Ho, C. C., and Zydney, A. L., *J. Membrane Sci.* **155,** 261 (1999).
13. Mochizuki, S., and Zydney, A. L., *J. Colloid Interface Sci.* **158**(1), 136 (1993).
14. Hermia, J., *Trans. Inst. Chem. Eng.* **60,** 183 (1982).
15. Porter, M. C., "AIChE Symp. Ser. No. 171." American Institute of Chemical Engineers, New York, 1977.
16. Belter, P. A., Cussler, E. L., and Hu, W. S., "Bioseparations—Downstream Processing for Biotechnology." Wiley, New York, 1988.
17. Opong, W. S., and Zydney, A. L., *J. Colloid Interface Sci.* **142,** 41 (1991).